Supplementary Information

Rapid detection and identification of vancomycin sensitive bacteria using an electrochemical apta-sensor

Zorica Novakovic[1], Majd Khalife[2], Vlad Costache[2,3], Maria Joao Camacho[4], Veronica Martins[4], Susana Cardoso[4], Ivana Gadjanski[1], Marko Radovic[1], Jasmina Vidic[2,].*

[1]University of Novi Sad, BioSense Institute, 21000 Novi Sad, Serbia.

[2]Université Paris-Saclay, INRAE, AgroParisTech, Micalis Institute, UMR 1319, 78350 Jouy-en-Josas, France.

[3]MIMA2 Imaging Core Facility, Microscopie et Imagerie des Microorganismes, Animaux et Aliments, INRAE, 78350, Jouy-en-Josas, France.

[4]INESC Microsistemas e Nanotecnologias Rua Alves Redol, Lisbon, Portugal.

*, Corresponding author, jasmina.vidic@inrae.fr

a)

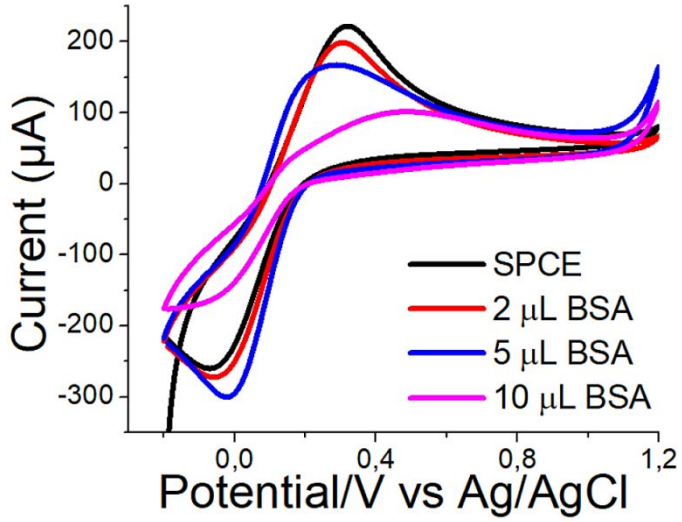

b)

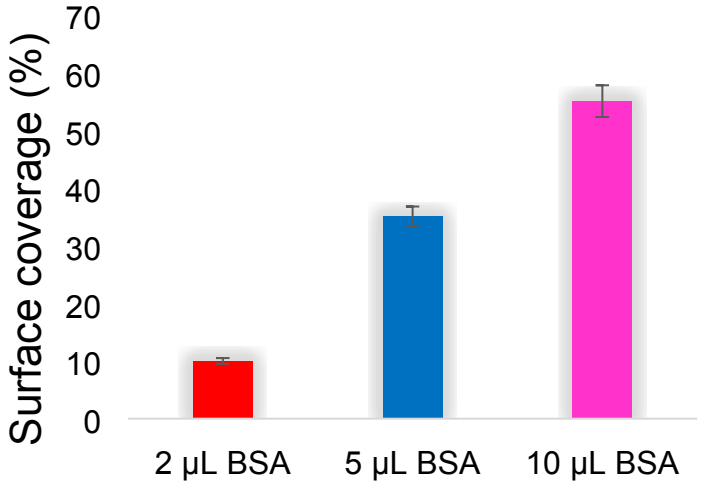

Figure S1. BSA immobilization. a) CV obtained using electrode incubated with different volumes of 2 mg/mL BSA. b) Surface coverage (%) versus different volumes of BSA used for functionalization.

a)

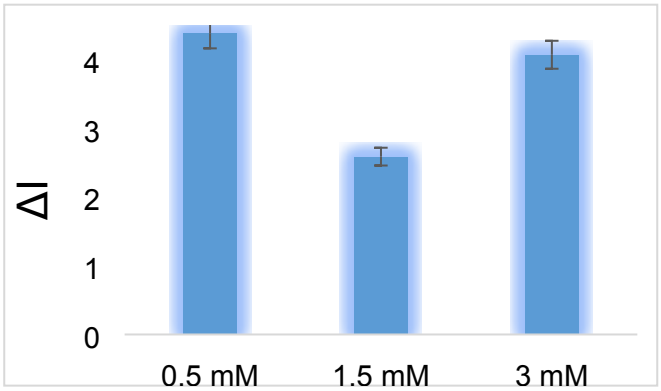

b)

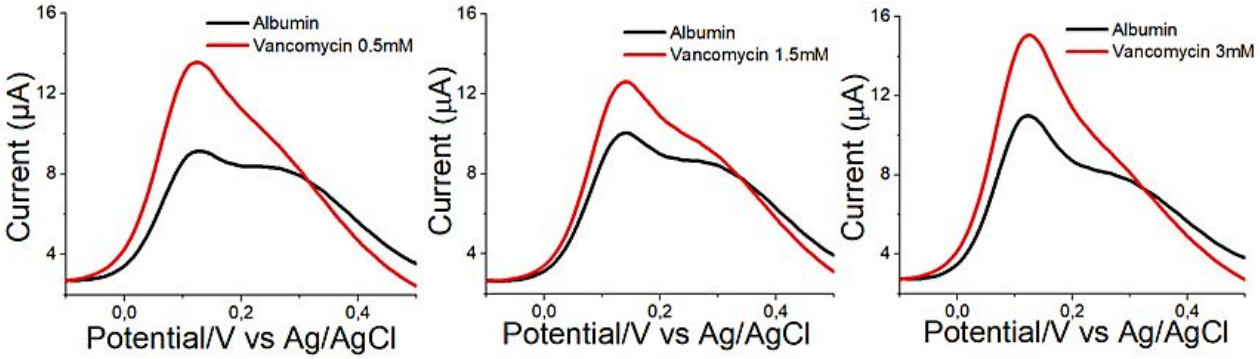

Figure S2. Vancomycin immobilization: optimization of concentration. a) The change in current intensity obtained after electrode incubation with different vancomycin concentrations. b) DPV obtained for different vancomycin concentrations. DPV parameters: potential ranged from -0.2 V to 0.5V, pulse amplitude 0.02 V.

a)

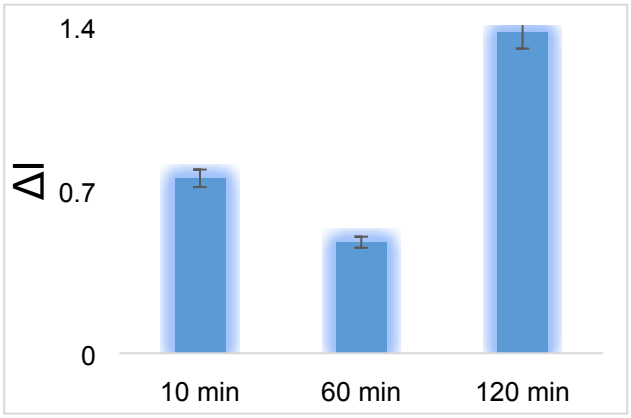

b)

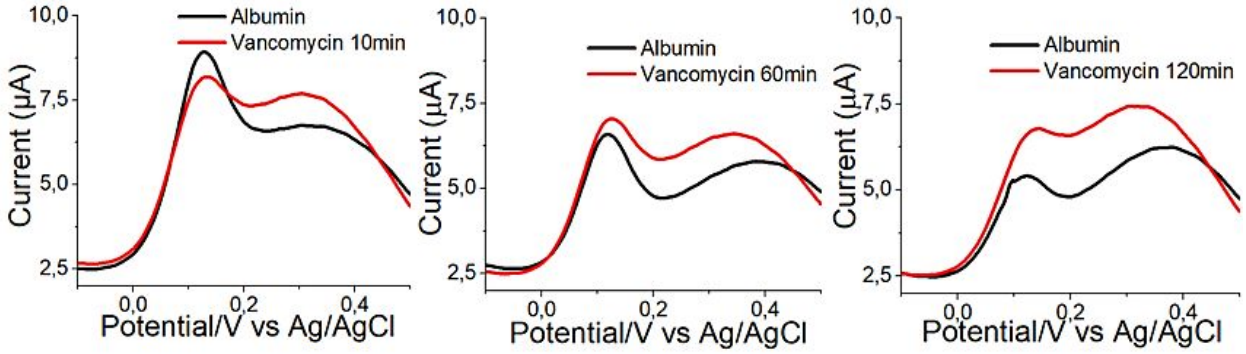

Figure S3. Vancomycin immobilization: optimization of incubation time. a) DPV current intensity versus different times of vancomycin incubation onto the working electrode. b) DPV obtained after the addition of vancomycin for different times of incubations.

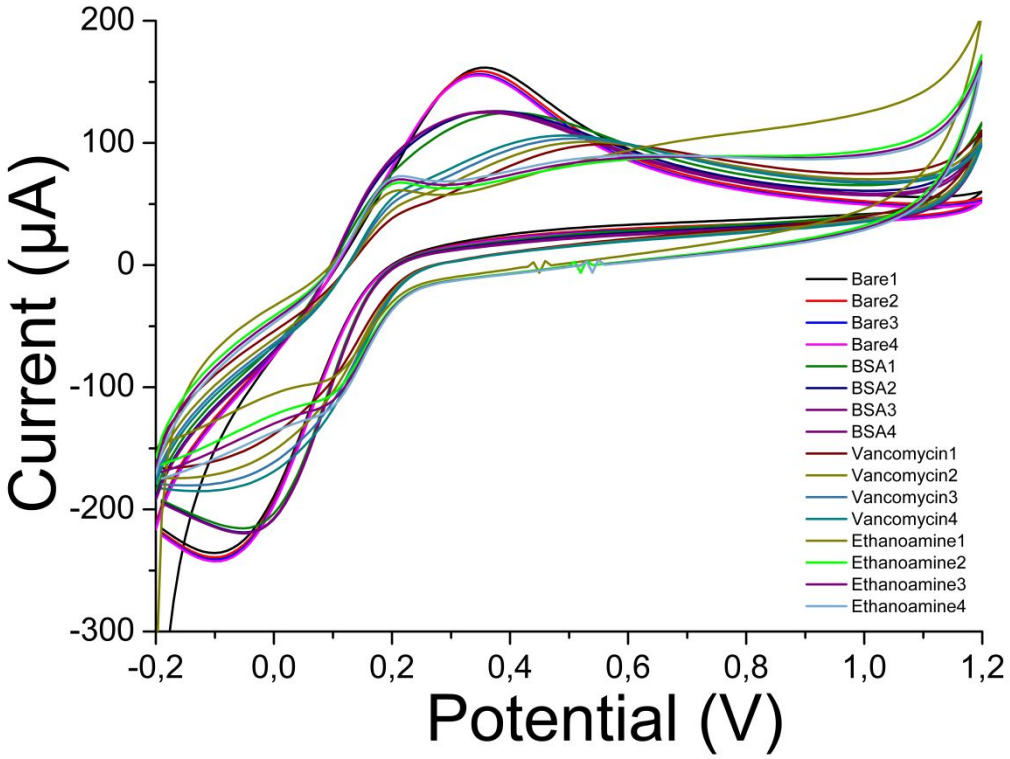

Figure S4. Electrode stability tests using CV at scan rate of 50 mV/s in $Fe^{2+/3+}$ redox couple in 0.1 KCl as supporting electrolyte.

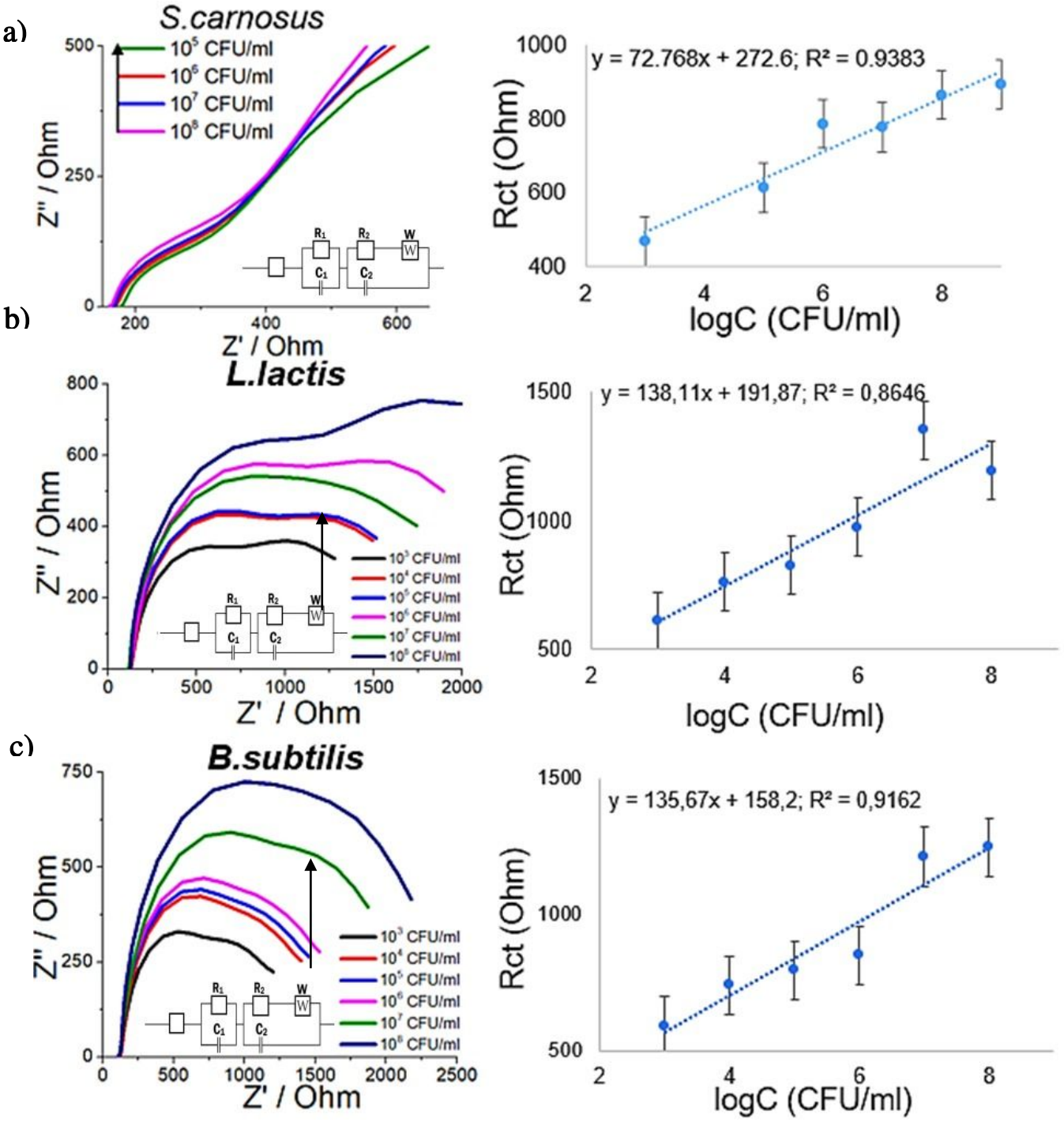

Figure S5. Electrochemical impedance spectroscopy measurements. a) Nyquist plot of impedance spectra of the vancomycin-based biosensor obtained from the increasing amount of *S. carnosus*, gram–positive bacteria in PBS. The calibration plot showing the change of charge transfer resistance, R_{ct}, as a function of the different concentrations of *S. carnosus*; b) and c) Nyquist plots of impedance spectra of *L. lactis* and *B. subtilis*, respectively.

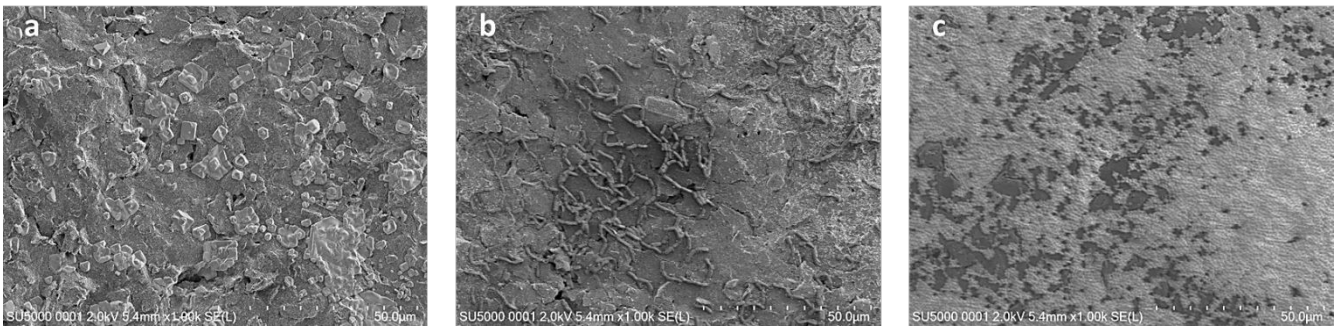

S6. SEM images of electrodes carrying vancomycin after incubation with *E. coli* (a), *B. cereus* (b) and *S. carnosus* (c) showing the nonadherence of *E. coli* in contrast to two Gram-positive bacteria.

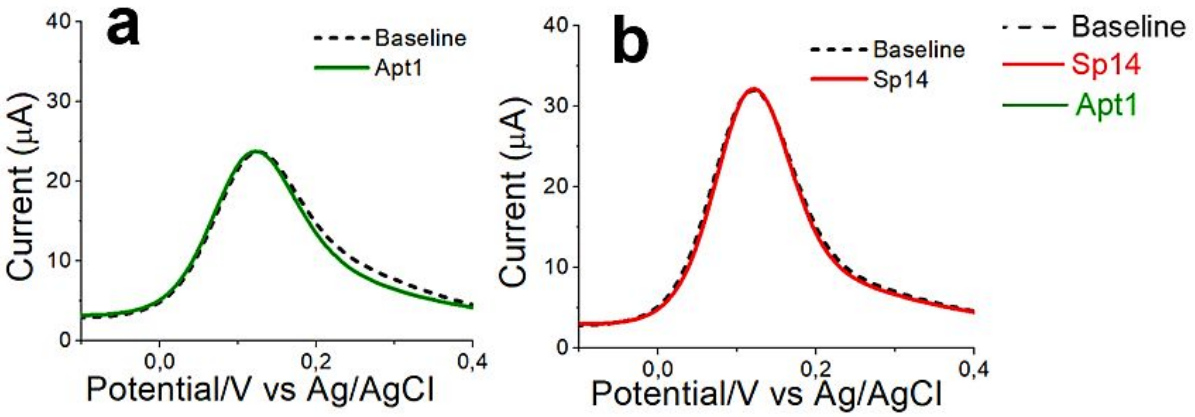

Figure S7. Aptamer background signal. a) DPV obtained after biosensor incubation with 10 μM Apt1; b) DPV obtained after biosensor incubation with 1 μM specific aptamer, Sp14.

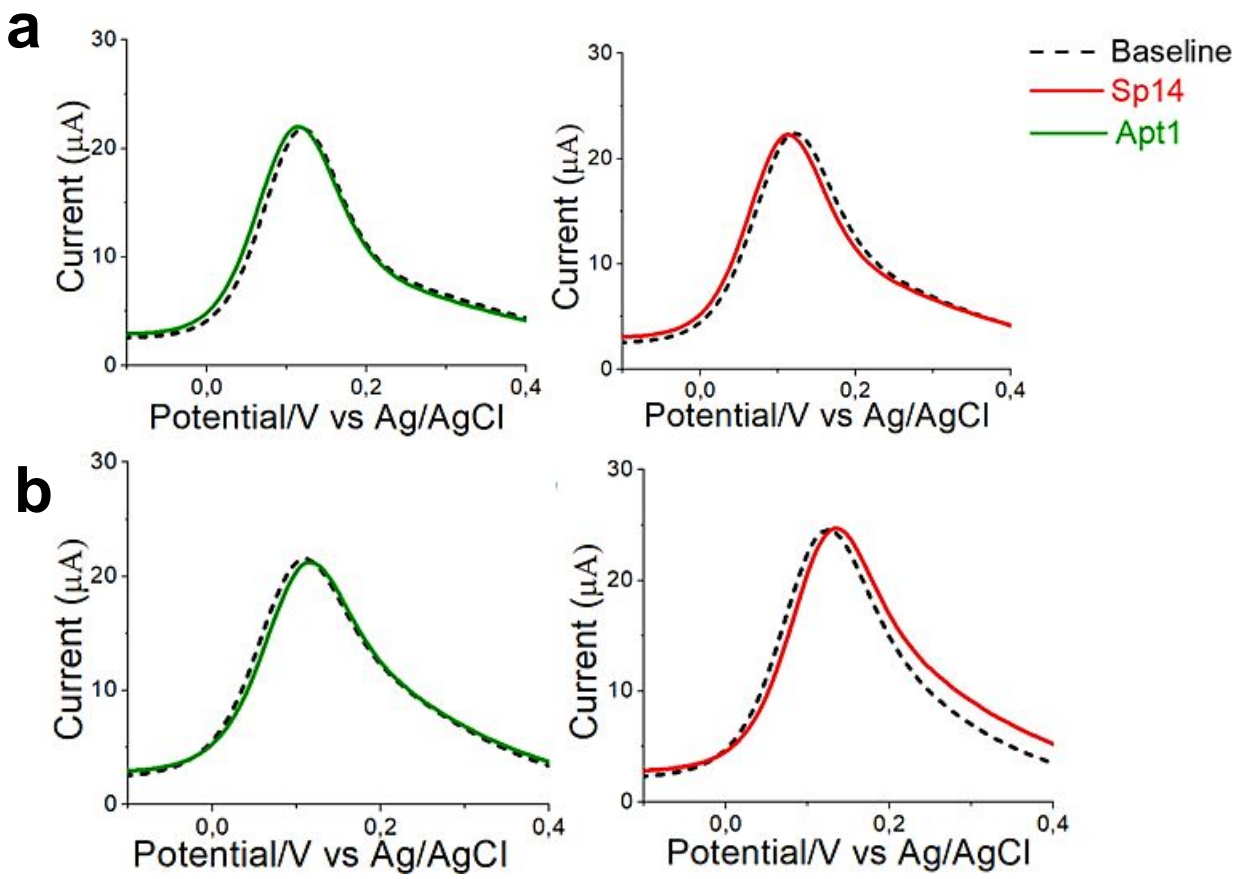

Figure S8. Aptamer background signal in real samples. a) DPV obtained after biosensor incubation with 10 μM Apt1 and 1 μM specific aptamer, Sp14 in milk; b) DPV obtained after biosensor incubation with 10 μM Apt1 and 1 μM specific aptamer, Sp14 in serum.

Table S1. Fitting values of the equivalent circuit elements for Gram positive bacteria detection by EIS Analyzer software. R1 is the internal resistance of the electrolyte solution, R2 is the resistance due to electrochemical reactions, R3 is the charge transfer resistance, and W1, the Warburg resistance.

	logC of bacteria	R_1	R_2	R_3	W
B. subtilis	3	127.05	588.86	810.65	/
	4	127.23	738.97	919.9	/
	5	120.42	794.61	881.12	/
	6	120.88	848.69	894.83	/
	7	121.72	1210	934.4	/
	8	124.85	1245.1	1172.8	/
L. lactis	3	125.42	608.5	1081.4	/
	4	125.06	760.43	1254.8	/
	5	126.7	825.24	1225.8	/
	6	118.28	973.71	1496.6	/
	7	124.56	1347.9	1743.3	/
	8	125,00	1193.1	1768.6	/
B. cereus	3	156.05	2123.5	231.7	$1.31E^{-19}$
	4	150.01	2153.6	284.22	$5.14E^{-19}$
	5	151.3	2362.5	235.98	$8.95E^{-19}$
	6	159.86	2518.2	265.27	$1.45E^{-18}$
	7	160	2597.9	231.78	$2.11E^{-18}$
S. carnosus	3	178.89	1628,5	155,78	$5.7484E^{-23}$
	4	168.57	1932,6	186,91	$1.3653E^{-22}$
	5	166.36	2204,4	188,73	$2.94E^{-20}$
	6	175.39	2627,6	230,18	$1.4154E^{-22}$
	7	162.13	2695,6	221,41	$3.0636E^{-22}$
S. aureus	3	124.41	238.51	367.82	324.87
	4	114.94	470.99	341.96	340.02
	5	122.85	423.1	602.99	359.95
	6	122.03	585.35	465.28	357.46
	7	121.49	585.35	499.46	367.2
	8	123.18	702.08	580.21	376.38